

---

# Emergent behaviour in large electrical networks

D. P. Almond, C. J. Budd, and N. J. McCullen

Bath Institute for Complex Systems, University of Bath, BA2 7AY, UK

**Summary.** Many complex systems have emergent behaviour which results from the way in that the components of the system interact, rather than their individual properties. However, it is often unclear as to what this emergent behaviour can be, or indeed how large the system should be for such behaviour to arise. In this paper we will address these problems for the specific case of an electrical network comprising a mixture of resistive and reactive elements. Using this model we will show, using some spectral theory, the types of emergent behaviour that we expect and also how large a system we need for this to be observed.

## 1 Introduction and Overview

The theory of complex systems offers great potential as a way of describing and understanding many phenomena involving large numbers of interacting agents, varying from physical systems (such as the weather) to biological and social systems [1]. A system is *complex* rather than just *complicated* if the individual components interact strongly and the resulting system behaviour is a product more of these interactions than of the individual components. Such behaviour is generally termed *emergent behaviour* and we can colloquially say that the complex system is demonstrating behaviour which is *more than the sum of its parts*. However, such descriptions of complexity are really rather vague and leave open many scientific questions. These include: how large does a system need to be before it is complex, what sort of interactions lead to emergent behaviour, and can the types of emergent behaviour be classified. More generally, how can we analyse a complex system? We do not believe that these questions can be answered *in general*, however, we can find answers to them in the context of specific complex problems. This is the purpose of this paper, which will study a complex system comprising a large binary electrical network, which can be used to model certain material behaviours.

Such large binary networks comprise disordered mixtures of two different but interacting components. These, arise both directly, in electrical circuits [2],[3],

[4], or mechanical structures [5], and as models of other systems such as disordered materials with varying electrical [6], thermal or mechanical properties in the micro-scale which are then coupled at a meso-scale. Many systems of condensed matter have this form [7],[8], [9]. Significantly, such systems are often observed to have *macroscopic emergent properties* which can have *emergent power-law behaviour* over a wide range of parameter values which is different from any power law behaviour of the individual elements of the network, and is a product of the way in which the responses of the components *combine*. As an example of such a binary disordered network, we consider a (set of random realisations of a) binary network comprising a random mixture with a proportion of  $(1 - p)$  resistors with frequency independent admittance  $1/R$  and  $p$  capacitors with complex admittance  $i\omega C$  directly proportional to frequency  $\omega$ . This network when subjected to an applied alternating voltage of frequency  $\omega$  has a the total admittance  $Y(\omega)$ . We observe that over a wide range of frequencies  $0 < \omega_1 < \omega < \omega_2$ , the admittance displays *power law emergent characteristics*, so that  $|Y|$  is proportional to  $\omega^\alpha$ , for an appropriate exponent  $\alpha$ . Significantly,  $\alpha$  is not equal to zero or one (the power law of the response of the individual circuit elements) but depends upon the proportion of the capacitors in the network. For example when this proportion takes the *critical value* of  $p = 1/2$ , then  $\alpha = 1/2$ . The effects of network size, and component proportion, are important in that  $\omega_1$  and  $\omega_2$  depend upon both  $p$  and  $N$ . In the case of  $p = 1/2$  this is a strong dependence and we will see that  $\omega_1$  is inversely proportional to  $N$  and  $\omega_2$  directly proportional to  $N$ , as  $N$  increases to infinity. It is in this frequency range that both the resistors and capacitors share the (many) current paths through the network, and they interact strongly. The emergent behaviour is a result of this interaction. For  $0 < \omega < \omega_1$  and  $\omega > \omega_2$  we see a transition in the behaviour. In these ranges either the resistors or the capacitors act as conductors, and there are infrequent current paths, best described by percolation theory. In these ranges the emergent power law behaviour changes and we see instead the individual component responses. Hence we see in this example of a complex system (i) an emergent region with a power law response depending on the proportion but not the arrangement or number of the components (ii) a more random percolation region with a response dominated by that of individual components and (iii) a transition between these two regions at frequency values which depends on the number and proportion of components in the system. The purpose of this paper is to partly explain this behaviour.

The layout of the remainder of this paper is as follows. In Section 2 we will give a series of numerical results which illustrate the various points made above on the nature of the network response. In Section 3 we will formulate the matrix equations describing the network and the associated representation of the admittance function in terms of poles and zeros. In Section 4 we will discuss, and derive, a series of statistical results concerning the distribution of the poles and zeros. In Section 5 we will use these statistical results to derive

the asymptotic form of the admittance  $|Y(\omega)|$  in the critical case of  $p = 1/2$ . In Section 6 we compare the asymptotic predictions with the numerical computations. Finally in Section 7 we will draw some conclusions from this work.

## 2 Simple Network Models and Their Responses

In this section we show the basic models for composite materials and associated random binary electrical networks, and present the graphs of their responses. In particular we will look in detail at the existence of a power law emergent region, and will obtain empirical evidence for the effects of network size  $N$  and capacitor proportion  $p$ , on both this region and the 'percolation behaviour' when  $CR\omega \ll 1$  and  $CR\omega \gg 1$ .

### 2.1 Modelling Composites as Complex Rectangular Networks

An initial motivation for studying binary networks comes from models of composite materials. Disordered two-phase composite materials are found to exhibit power-law scaling in their bulk responses over several orders of magnitude in the contrast ratio of the components [10], [3], and this effect has been observed [2],[11] in both physical and numerical experiments on conductor-dielectric composite materials. In the electrical experiments this was previously referred to as "Universal Dielectric Response" (UDR), and it has been observed [7],[8] that this is an emergent property arising out of the random nature of the mixture. A simple model of such a conductor-dielectric mixtures with fine structure is a large electrical circuit replacing the constituent conducting and dielectric parts with a linear C-R network of  $N \gg 1$  resistors and capacitors, respectively as illustrated in Figure 1. For a binary disordered mixture, the different components can be assigned randomly to bonds on a lattice [12]. with bonds assigned randomly as either C or R, with probability  $p$ ,  $1 - p$  respectively. The components are distributed in a two-dimensional lattice between two bus-bars. One of which is grounded and the other is raised to a potential  $V(t) = V \exp(i\omega t)$ . This leads to a current  $I(t) = I(\omega) \exp(i\omega t)$  between the bus-bars, and we measure the macroscopic (complex) admittance given by  $Y(\omega) = I(\omega)/V$ . A large review of this and binary disordered networks can be found in [13, 3].

We now present an overview of the results found for the admittance conduction of the C-R network, explaining the PLER and its bounds. In particular we need to understand the difference between percolation behaviour and power law emergent behaviour. To motivate these results we consider initially the cases of very low and very large frequency.



this implies that if  $p = 1/2$  then there are *four possible qualitatively different* types of response for any random realisation of the system.

For *intermediate values* of  $\omega$  the values of the admittance of the resistors and the capacitors are much closer to each other and there are many current paths through the network, In Figure2 we see the current paths in the three cases of (a) percolation, (b) transition between percolation and emergence (c) emergence.

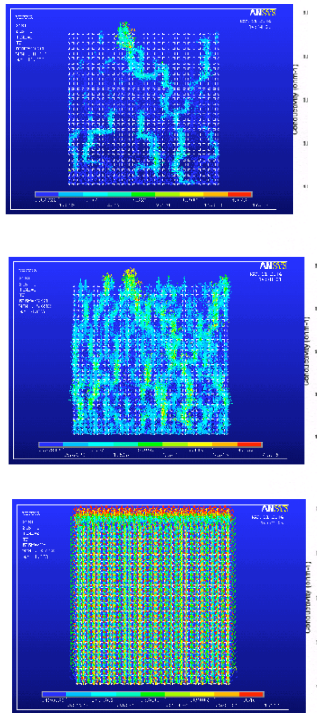


**Fig. 2.** An illustration of the three different types of current path observed in the percolation, transition and emergent regions.

The emergence region has power-law emergent behaviour. This is characterised by two features: (i) an admittance response that is proportional to  $\omega^\alpha$  for some  $0 < \alpha < 1$  over a range  $\omega \in (\omega_1, \omega_2)$ . (ii) In the case of  $p = 1/2$  a response that is not randomly dependent upon the network configuration.

Figures (3) and (4) plot the admittance response as a function of  $\omega$  in the cases of  $p = 0.4$ ,  $p = 0.6$  and  $p = 1/2$ . The figures clearly demonstrate the forms of behaviour described above. Observe that in all cases we see quite a sharp transition between the percolation type behaviour and the emergent power law behaviour as  $\omega$  varies.

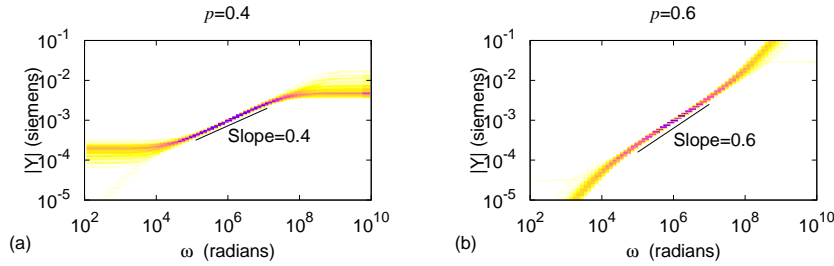


**Fig. 3.** Typical responses of network simulations for values of  $p \neq 1/2$  which give qualitatively different behaviour so that in the percolation region with  $CR \omega \ll 1$  or  $CR \omega \gg 1$ , we see resistive behaviour in case (a) and capacitive behaviour in case (b). The figures presented are density plots of 100 random realisations for a  $20 \times 20$  network. Note that all of the realisations give very similar results.

### The effects of network size $N$ and capacitor proportion $p$ .

We have seen above how the response of the network depends strongly upon  $p$ . It also depends (more weakly) upon the network size  $N$ . Figure 5 shows the response for the critical value of  $p = 1/2$  for different values of  $N$ . Observe that in this case the width of the power-law emergent region increases apparently without bound, as  $N$  increases, as do the magnitude of the responses for small and large frequencies. In contrast in Figure (6) we plot the response for  $p = 0.4$  and again increase  $N$ . In contrast to the former case, away from the critical percolation probability the size of the power-law emergent region appears to scale with  $N$  for small  $N$  before becoming asymptotic to a finite value for larger values of  $N$ .

These results are consistent with the predictions of the Effective-Medium-Approximation (EMA) calculation [16],[3] which uses a homogenisation argument to determine the response of a network with an infinite number ( $N = \infty$ ) of components. In particular, the EMA calculation predicts that in this limiting case, the response for  $p = 1/2$  is always proportional to  $\sqrt{\omega}$  and that it  $p < 1/2$  then the response is asymptotic to  $\epsilon \equiv 1/2 - p$  as  $\omega \rightarrow 0$  and to  $1/\epsilon$  as  $\omega \rightarrow \infty$ . However the EMA calculation does not include the effects of the network size.

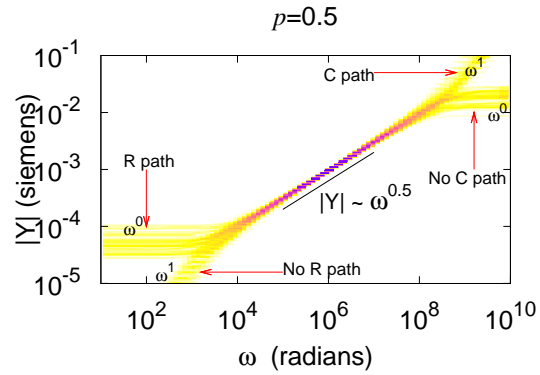


**Fig. 4.** Responses for 100 realisations at  $p = 1/2$  showing four different qualitative types of response for different realisations. Here, about half of the responses have a resistive percolation path and half have a capacitive one at low frequencies with a similar behaviour at high frequencies. The responses at high and low values of  $CR\omega$  indicate which of these cases exist for a particular realisation. The power-law emergent region can also be seen in which the admittance scales as  $\sqrt{\omega}$  and all of the responses of the different network realisations coincide

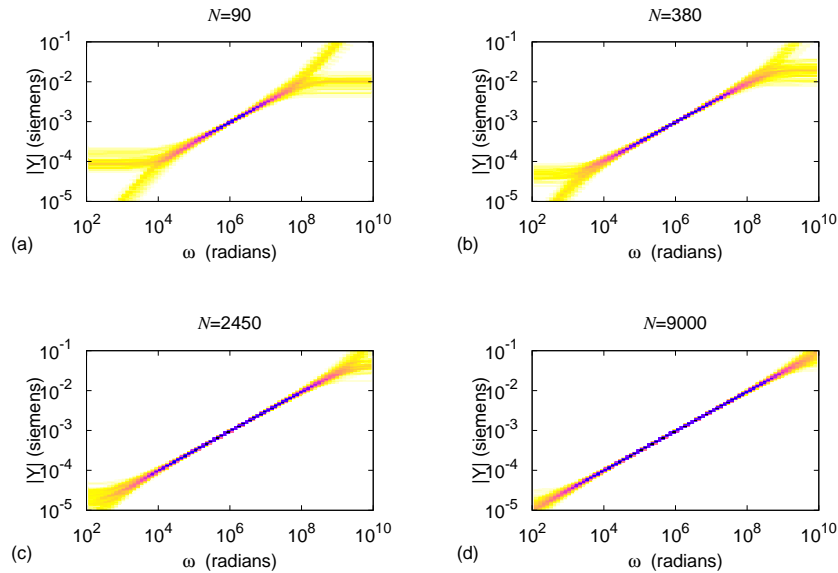


**Fig. 5.** The effect of network size  $N$  on the width of the power-law emergent region for  $p = 1/2$ , in which we see this region increasing without bound.

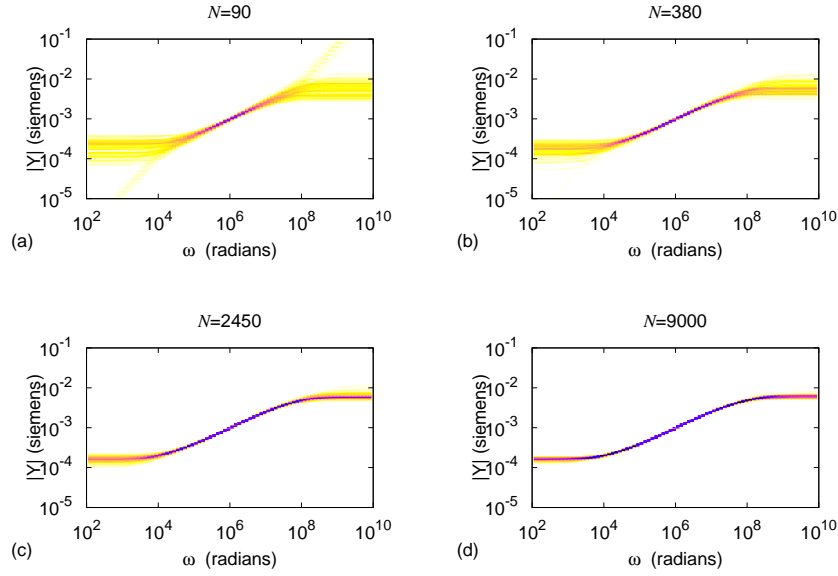


**Fig. 6.** The effect of the network size  $N$  on the power-law emergent region for  $p = 0.4$ , in which we see this region becoming asymptotic to a finite set as  $N \rightarrow \infty$ .

To compare and contrast these results, we consider for  $p \leq 1/2$ , the *dynamic range* of the response for those realisations which have a resistive solution for both low and high frequencies (that is with probability one if  $p < 1/2$  and probability  $1/4$  if  $p = 1/2$ ). We define the dynamic range to be

$$\hat{Y} = \frac{|Y|_{max}}{|Y|_{min}} = \frac{|Y(\infty)|}{|Y(0)|}.$$

In Figure (7) we plot  $\hat{Y}$  as a function of  $N$  for a variety of values of  $p \leq 1/2$ . We see from this figure that if  $p = 1/2$  then  $\hat{Y}$  is directly proportional to  $N$  for all values of  $N$  plotted. In contrast, if  $p < 1/2$  then  $\hat{Y}$  is directly proportional to  $N$  for smaller values of  $N$  and then becomes asymptotic to a finite value  $\hat{Y}(p)$  as  $N \rightarrow \infty$ .

### 3 Linear circuit analysis of the network

We now describe in detail how the disordered material is modelled by a general network model. In this we consider two components of admittance  $y_1$  and  $y_2$  so that the proportion of the first component is  $(1 - p)$  and the second is  $p$ . These will have admittance ratio  $\mu = \frac{y_2}{y_1}$ . For a capacitor-resistor (C-R)

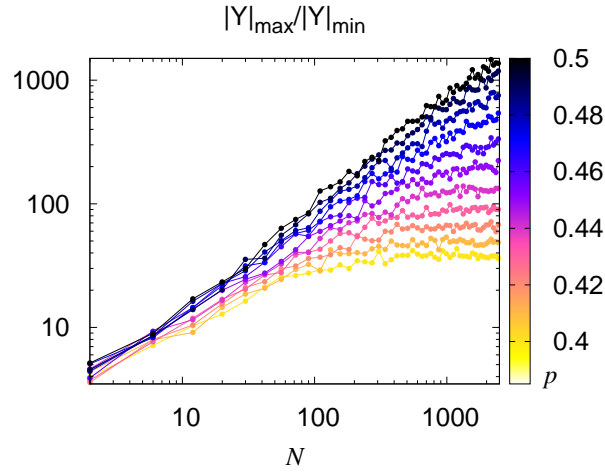


**Fig. 7.** The variation of the dynamic range  $\hat{Y} = |Y|_{max}/|Y|_{min}$  as a function of  $N$  and  $p$ .

network with a proportion  $p$  of capacitors with admittance  $y_2 = i\omega C$  and resistors admittance  $y_1 = 1/R$  we have

$$\mu = i\omega CR \text{ is purely imaginary.} \quad (1)$$

### 3.1 Linear Circuit Formulation

Now consider a 2D  $N$  node square lattice network, with all of the nodes on the left-hand-side (LHS) connected via a bus-bar to a time varying voltage  $V(t) = Ve^{i\omega t}$  and on the right-hand-side (RHS) via a bus-bar to earth (0V). We assign a (time-varying) voltage  $v_i$  with  $i = 1 \dots N$  to each (interior) node, and set  $\mathbf{v} = (v_1, v_2, v_3 \dots v_N)^T$  to be the vector of voltage unknowns. We will also assume that adjacent nodes are connected by a bond of admittance  $y_{i,j}$ . Here we assume further that  $y_{i,j} = y_1$  with probability  $1 - p$  and  $y_{i,j} = y_2$  with probability  $p$ . From Kirchhoff's current law, at any node all currents must sum to zero, so there are no sinks or sources of current other than at the boundaries. In particular, the current from the node  $i$  to an adjoining node at  $j$  is given by  $I_{i,j}$  where

$$I_{i,j} = (v_i - v_j)y_{i,j}.$$

It then follows that if  $i$  is *fixed* and  $j$  is allowed to vary over the four nodes adjacent to the node at  $i$  then

$$\sum_j y_{i,j}(v_i - v_j) = 0. \quad (2)$$

If we consider all of the values of  $i$  then there will be certain values of  $i$  that correspond to nodes adjacent to one of the two boundaries. If  $i$  is a node adjacent to the *left* boundary then certain of the terms  $v_j$  in (2) will take the value of the (known) applied voltage  $V(t)$ . Similarly, if a node is adjacent to the right hand boundary then certain of the terms  $v_j$  in (2) will take the value of the ground voltage 0. Combining all of these equations together leads to a system of the form

$$K\mathbf{v} = V(t)\mathbf{b} = Ve^{i\omega t}\mathbf{b}, \quad (3)$$

where  $K \equiv K(\omega)$  is the (constant in time)  $N \times N$  *sparse symmetric Kirchoff matrix* for the system formed by combining the individual systems (2), and the adjacency vector  $\mathbf{b} \equiv \mathbf{b}(\omega)$  is the vector of the admittances of the bonds between the left hand boundary and those nodes which connected to this boundary, with zero entries for all other nodes. As this is a *linear system*, we can take

$$\mathbf{v} = \mathbf{V}e^{i\omega t}$$

so that the (constant in time) vector  $\mathbf{V}$  satisfies the linear algebraic equation

$$K\mathbf{V} = V\mathbf{b}. \quad (4)$$

If we consider the total current flow  $I$  from the LHS boundary to the RHS boundary then we have

$$I = \mathbf{b}^T(V\mathbf{e} - \mathbf{V}) \equiv \mathbf{b}^T\mathbf{V} - Vc$$

where  $\mathbf{e}$  is the vector comprising ones for those nodes adjacent to the left boundary and zeroes otherwise and  $c = \mathbf{b}^T\mathbf{V}$ . Combining these expressions, the equations describing the system are then given by

$$K\mathbf{V} - \mathbf{b}V \equiv \mathbf{0}, \quad cV - \mathbf{b}^T\mathbf{V} = I. \quad (5)$$

The *bulk admittance*  $Y(\mu)$  of the whole system is then given by  $Y = I/V$  so that

$$Y(\mu) = c - \mathbf{b}^TK^{-1}\mathbf{b}. \quad (6)$$

Significantly, the symmetric Kirchoff matrix  $K$  can be separated into the two sparse symmetric  $N \times N$  component matrices  $K = K_1 + K_2$  which correspond to the conductance paths along the bonds occupied by each of the two types of components. Furthermore

$$K_1 = y_1L_1 \quad \text{and} \quad K_2 = y_2L_2 = \mu y_1L_2 \quad (7)$$

where the terms of the sparse symmetric connectivity matrices  $L_1$  and  $L_2$  are constant and take the values  $-1, 0, 1, 2, 3, 4$ . Note that  $K$  is a *linear affine function* of  $\mu$ . Furthermore,

$$\Delta = L_1 + L_2$$

is the discrete (negative definite symmetric) Laplacian for a 2D lattice. Similarly we can decompose the adjacency vector into two components  $\mathbf{b}_1$  and  $\mathbf{b}_2$  so that

$$\mathbf{b} = \mathbf{b}_1 + \mathbf{b}_2 = y_1 \mathbf{e}_1 + y_2 \mathbf{e}_2$$

where  $\mathbf{e}_1$  and  $\mathbf{e}_2$  are *orthogonal vectors* comprising ones and zeros only corresponding to the two bond types adjacent to the LHS boundary. Observe again that  $\mathbf{b}$  is a linear affine function of  $\mu$ . A similar decomposition can be applied to the scalar  $c = c_1 + \mu c_2$ .

### 3.2 Poles and Zeroes of the Admittance Function

To derive formulæ for the expected admittances in terms of the admittance ratio  $\mu = i\omega CR$  we now examine the structure of the admittance function  $Y(\mu)$ . As the matrix  $K$ , the adjacency vector  $\mathbf{b}$  and the scalar  $c$  are all affine functions of the parameter  $\mu$  it follows immediately from Cramer's rule applied to (5) that the admittance of the network  $Y(\mu)$  is a rational function of the parameter  $\mu$ , taking the form of the ratio of two complex polynomials  $P(\mu)$  and  $Q(\mu)$  of respective degrees  $r \leq N$  and  $s \leq N$ , so that

$$Y(\mu) = \frac{Q(\mu)}{P(\mu)} = \frac{q_0 + q_1\mu + q_2\mu^2 + \dots + q_r\mu^r}{p_0 + p_1\mu + p_2\mu^2 + \dots + p_s\mu^s} \quad (8)$$

We require that  $p_0 \neq 0$  so that the response is physically realisable, with  $Y(\mu)$  bounded as  $\omega$  and hence  $\mu \rightarrow 0$ . Several properties of the network can be immediately deduced from this formula. First consider the case of  $\omega$  *small*, so that  $\mu = i\omega CR$  is also small. From the discussions in Section 2, we predict that either there is (a) a resistive percolation path in which case  $Y(\mu) \sim \mu^0$  as  $\mu \rightarrow 0$  or (b) such a path does not exist, so that the conduction is capacitive with  $Y(\mu) \sim \mu$  as  $\mu \rightarrow 0$ . The case (a) arises when  $p_0 \neq 0$  and the case (b) when  $q_0 = 0$ . Observe that this implies that the absence of a resistive percolation path as  $\mu \rightarrow 0$  is equivalent to the polynomial  $Q(\mu)$  *having a zero when  $\mu = 0$* . Next consider the case of  $\omega$  and hence  $\mu$  large. In this case

$$Y(\mu) \sim \frac{q_r}{p_s} \mu^{r-s} \quad \text{as } \mu \rightarrow \infty.$$

Again we may have (c) a resistive percolation path at high frequency with response  $Y(\mu) \sim \mu^0$  as  $\mu \rightarrow \infty$ , or a capacitive path with  $Y(\mu) \sim \mu$ . In case (c) we have  $s = r$  and  $p_r \neq 0$  and in case (d) we have  $s = r - 1$  so that we can think of taking  $p_r = 0$ . Accordingly, we identify four types of network defined in terms of these percolation paths for low and high frequencies, which correspond to the cases (a),(b),(c),(d) so that

(a)	$p_0 \neq 0$
(b)	$p_0 = 0$
(c)	$p_r \neq 0$
(d)	$p_r = 0$

The polynomials  $P(\mu)$  and  $Q(\mu)$  can be factorised by determining their respective roots  $\mu_{p,k}, k = 1 \dots s$  and  $\mu_{z,k}, k = 1 \dots r$  which are the *poles and zeroes* of the network. We will collectively call these zeroes and poles the *resonances* of the network. It will become apparent that the emergent response of the network is in fact a manifestation of certain regularities of the locations of these resonances. Note that in Case (b) we have  $\mu_{z,1} = 0$ . Accordingly the network admittance can be expressed as

$$Y(\mu, N) = D(N) \frac{\prod_{k=1}^r (\mu - \mu_{z,k})}{\prod_{k=1}^s (\mu - \mu_{p,k})}. \quad (9)$$

Here  $D(N)$  is a function which does not depend on  $\mu$  but does depend on the characteristics of the network.

It is a feature of the stability of the network (bounded response), and the affine structure of the symmetric linear equations which describe it [3], that the poles and zeros of  $Y(\mu)$  are all *negative real numbers, and interlace* so that

$$0 \geq \mu_{z,1} > \mu_{p,1} > \mu_{z,2} > \mu_{p,2} \dots > \mu_{z,s} > \mu_{p,s} (> \mu_{z,r}) \quad (10)$$

Because of this, we may recast the equation (11) in terms of  $\omega$  so that

$$|Y(\mu, N)| = |D(N)| \frac{\prod_{k=1}^r |\omega - iW_{z,k}|}{\prod_{k=1}^s |\omega - iW_{p,k}|} \quad (11)$$

where  $W_{z,k} \geq 0, W_{p,k} > 0$ .

## 4 The distribution of the resonances

The previous section has described the network response in terms of the location of the poles and the zeros. We now consider the statistical distribution of these values and claim that it is this distribution which leads to the observed emergent behaviour. We note that if we consider the elements of the network to be assigned randomly (with the components taking each of the two possible values with probabilities  $p$  and  $1-p$  then we can consider the resonances to be random variables. There are three interesting questions to ask, which become relevant for the calculations in the next section, namely

1. What is the statistical distribution of  $W_{p,k}$  if  $N$  is large.
2. Given that the zeros interlace the poles, what is the statistical distribution of the location of a zero between its two adjacent poles.
3. What are the ranges of  $W_{p,k}$ , in particular, how do  $W_{p,1}$  and  $W_{p,N}$  vary with  $N$  and  $p$ .

In each case we will find good numerical evidence for strong statistical regularity of the poles, especially in the critical case of  $p = 1/2$ , leading to partial answers to each of the above questions. For the remainder of this paper we will now only consider this critical case.

#### 4.1 Pole location

In the critical case, the two matrices  $L_1$  and  $L_2$  representing the connectivity of the two components, have a statistical duality, so that any realisation which leads to a particular matrix  $L_1$  is equally likely to lead to the same matrix  $L_2$ . Because of this, if  $\mu$  is an observed eigenvalue of the pair  $(L_1, L_2)$  then it is equally likely for there to be an observed eigenvalue of the pair  $(L_2, L_1)$ . The latter being precisely  $1/\mu$ . Thus in any set of realisations of the system we expect to see the eigenvalues  $\mu$  and  $1/\mu$  occurring with equal likelihood. It follows from this simple observation that the variable  $\log|\mu|$  should be expected to have a symmetric probability distribution with mean zero. Applying the central limit theorem in this case leads to the expectation that  $\log|\mu|$  should follow a normal distribution with mean zero (so that  $\mu$  has a *log-normal* distribution centred on  $\mu = -1$ ). Similarly, if  $\mu_1$  is the smallest value of  $\mu$  and  $\mu_N$  the largest value then  $\mu_1 = -1/\mu_N$ . In fact we will find that in this case of  $p = 1/2$  we have  $\mu_1 \sim -1/N$  and  $\mu_N \sim -N$ . In terms of the frequency response, as  $\mu_{p,k} = -CR W_{p,k}$ , it follows that  $\log(W_{p,k})$  is expected to have a mean value of  $-\log(CR)$ . Following this initial discussion, we now consider some actual numerical computations of the distribution of the poles in a C-R network for which  $CR = 10^{-6}$  so that  $-\log_{10}(CR) = 6$ . We take a single realisation of a network with  $N \approx 380$  nodes, and determine the location of  $CR W_{p,k}$  for this case. We then plot the location of the logarithm of the poles as a function of  $k$ . The results are given in Fig 8 for the case of  $p = 1/2$ . Two features of this figure are immediately obvious. Firstly, the terms  $W_{p,k}$  appear to be the point values of a regular function  $f(k)$ . Secondly, as predicted above, the logarithm of the pole location shows a strong degree of symmetry about zero. We compare the form of this graph with that of the inverse error function, that is we compare  $\text{erf}(\log(CR W_{pk}))$  with  $k$ . The correspondence is very good, strongly indicating that  $\log(f)$  takes the form of the inverse error function. .

#### 4.2 Pole-Zero Spacing

The above has considered the distribution of the poles. As a next calculation we consider the statistical distribution of the location of the zeros with respect

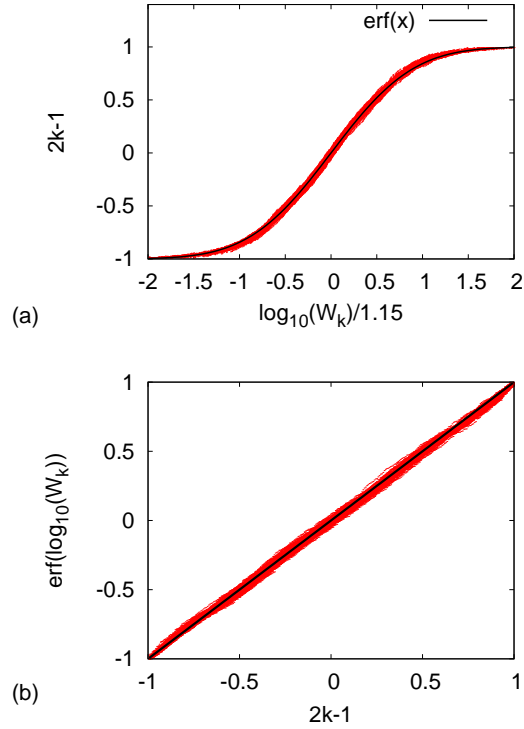


**Fig. 8.** The location of the logarithm of the poles as a function of  $k$  and a comparison with the inverse error function.

to the poles. In particular we consider the variable  $\delta_k$  given by

$$\delta_k \equiv \frac{W_{p,k} - W_{z,k}}{W_{p,k} - W_{p,k-1}} \tag{12}$$

which expresses the *relative location* of each zero in terms of the poles which it interlaces. In Figure 9 we plot the distribution of the mean value  $\bar{\delta}_k$  of  $\delta^k$  over 100 *realisations* of the network, plotted as a function of the mean location of  $\log(W_{p,k})$  for  $p = 1/2$ . This figure is remarkable as it indicates that when  $p = 1/2$  the mean value of  $\delta_k$  is equal to  $1/2$  almost independently of the value of  $\log(W_{p,k})$ . There is some deviation from this value at the high and low ends of the range, presumably due to the existence of the degenerate poles at zero and at infinity, and there is some evidence for a small asymmetry in the results, but the constancy of the mean near to  $1/2$  is very convincing. This shows a remarkable duality between the zeros and the poles in the case of  $p = 1/2$ , showing that not only do they interlace, but that on average the zeros are mid-way between the poles and the poles are mid-way between the zeros.

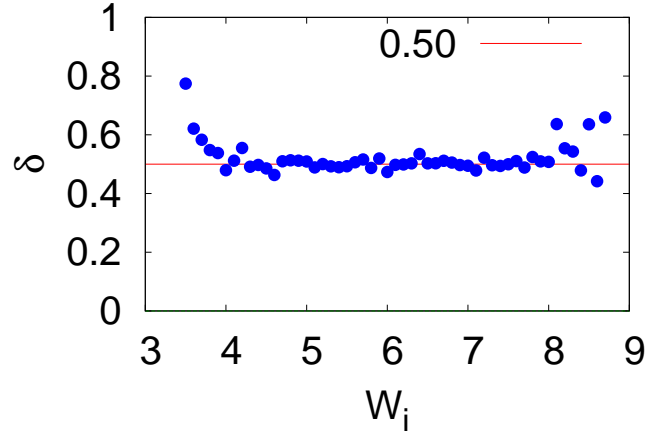


**Fig. 9.** Figure showing how the mean value  $\bar{\delta}_k$ , taken over many realisations of the critical network, varies with the mean value of  $\log(W_{p,k})$ .

### 4.3 Limiting Finite Resonances

Let  $N'$  be the number of *finite non-zero resonances*, the location of the first non-zero pole and zero be  $W_{z,1}, W_{p,1}$ , and the location of the last finite pole and zero be  $W_{p,N'}, W_{z,N'}$ . Observe that in the case of  $p = 1/2$  we expect a symmetrical relation so that  $W_{p,1}$  and  $W_{p,N'}$  might be expected to take reciprocal values. The value of  $N'$  can be considered statistically, and represents probability of a node contributing to the current paths and not being part of an isolated structure. Statistical arguments presented in [3] indicate that when  $p = 1/2$  this is given by

$$N' = 3 \left( 2 - \sqrt{3} \right) N = 0.804 \dots N.$$

We now consider the values of  $W_{p,1}$  and of  $W_{p,N'}$ . These will become very important when we look at the *transition between emergent type behaviour and percolation type behaviour* which is one of the objectives of this research. A log-log plot of the values of  $W_{z,1}, W_{p,1}$  and of  $W_{z,N'}, W_{p,N'}$  as functions of  $N$  for the case of  $p = 1/2$  is given in Figure 10. There is very clear evidence from these plots that each of  $W_{z,1}, W_{p,1}$  and  $W_{z,N'}, W_{p,N'}$  both have a *strong power law dependence* upon  $N$  for *all values of  $N$* . Indeed we have from a careful inspection of this figure that

$$W_{z,1}, W_{p,1} \sim N^{-1} \quad \text{and} \quad W_{z,N'}, W_{p,N'} \sim N.$$

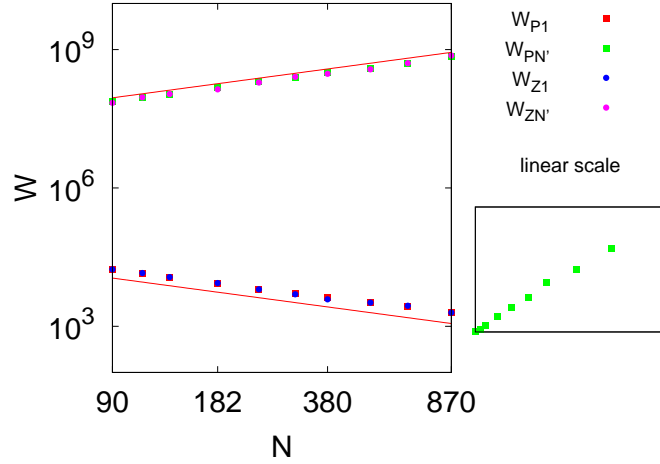


**Fig. 10.** Figure showing how the maximum pole and zero locations  $W_{p,N'}, W_{z,N'}$  scale as  $N$  and the minimum pole and zero locations  $W_{p,1}, W_{z,1}$  scale as  $1/N$ .

#### 4.4 Summary

The main conclusions of this section are that there is a strong statistical regularity in the location of the poles and the zeros of the admittance function. In particular we may make the following conclusions based on the calculations reported in this section.

1.  $W_{p,k} \sim f(k)$  for an appropriate continuous function  $f(k)$  where  $f$  depends upon  $N$  very weakly.
2. If  $p = 1/2$  and if  $W_{z,1} \neq 0$ , then

$$W_{1p}, W_{1z} \sim N^{-1}, \quad W_{N'p}, W_{N'z} \sim N.$$

3. If  $p = 1/2$  then  $\bar{\delta}_k \approx 1/2$ .

All of these conclusions point towards a good degree of statistical regularity in the pole distribution, and each can be justified to a certain extent by statistical and other arguments. We will now show how these statistical regularities lead to power law emergent region, and how this evolves into a percolation response.

### 5 Asymptotic Analysis of the Power Law Emergent Response

We will use the results in the summary of the previous section to derive the form of the conductance in the case of a critical C-R network. The formulae

that we derive will take one of four forms, depending upon the nature of the percolation paths for low and high frequencies.

### 5.1 Derivation of the response

We now consider the formulae for the absolute value of the admittance of the C-R network at a frequency of  $\omega$  given by

$$|Y(\omega)| = |D(N)| \frac{\prod_{k=1}^r |\omega - iW_{z,k}|}{\prod_{k=1}^s |\omega - iW_{p,k}|}$$

where the zero interlacing theorem implies that

$$0 \leq W_{z,1} < W_{p,2} < W_{z,2} < W_{2p} < \dots < W_{p,s} (< W_{z(s+1)}).$$

Here we assume that we have  $s = N'$  poles, but consider situations with different percolation responses at low and high frequencies depending upon whether the first zero  $W_{z,1} = 0$  and on the existence or not of there is a final zero  $W_{z,(N'+1)}$ . These four cases lead to four functional forms for the conductance, all of which are realisable in the case of  $p = 1/2$ . In this section we derive each of these four forms from some simple asymptotic arguments. At this stage the constant  $D(N)$  is undetermined, but we will be able to deduce its value from our subsequent analysis. Although simple, these arguments lead to remarkably accurate formulae when  $p = 1/2$ , when compared with the numerical calculations, that predict not only the PLER but also the limits of this region.

Simple trigonometric arguments imply that

$$|Y(\omega)| = |D(N)| \frac{\prod_{k=1}^r \sqrt{\omega^2 + W_{z,k}^2}}{\prod_{k=1}^s \sqrt{\omega^2 + W_{p,k}^2}} \quad (13)$$

To obtain an asymptotic formula from this identity, we will assume that  $s = N'$  is large, and that there is a *high density* of poles and zeros along the imaginary axis. From the results in the previous section we know that asymptotically the poles  $W_{p,k}$  follow a regular distribution and that the zeroes have a regular spacing between the poles. The conclusions of the previous section on the distribution of the poles and the zeros leads to the following formulae

$$\begin{aligned}
W_{p,k} &\sim f(k) \\
\frac{W_{p,(k+1)} - W_{z,k}}{W_{p,(k+1)} - W_{p,k}} &= \delta_k, \\
W_{p,(k+1)} - W_{pk} &\sim f'(k) \\
W_{z,(k+1)} &\sim f(k) + (1 - \delta_k)k f'(k)
\end{aligned}$$

Here, as we have seen, the function  $\log(f(k))$  is given by the inverse of the error function, but its precise form does not matter too much for the next calculation. To do this we firstly consider the contributions to the product in (13) which arise from the terms involving the first pole to the final zero, so that we consider the following product

$$P \equiv |D(N)| \prod_{k=1}^{N'} \frac{\sqrt{\omega^2 + W_{z,(k+1)}^2}}{\sqrt{\omega^2 + W_{p,k}^2}} \quad (14)$$

Note that this product has implicitly assumed the existence of a final zero  $W_{z,(N'+1)}$ . This contribution will be corrected in cases for which such a final zero does not exist. Using the results in (14), in particular on the mean spacing of the zeros between the poles, we may express  $P$  as

$$\begin{aligned}
P^2 &= |D(N)|^2 \prod_{k=1}^{N'} \frac{\omega^2 + (f(k) + (1 - \bar{\delta}_k)f'(k))^2}{\omega^2 + f^2(k)} \\
&= |D(N)|^2 \prod_{k=1}^{N'} \frac{\omega^2 + f^2(k) + 2(1 - \bar{\delta}_k)f(k)f'(k) + HOT}{\omega^2 + f^2(k)} \\
&= |D(N)|^2 \prod_{k=1}^{N'} 1 + \frac{2(1 - \bar{\delta}_k)f(k)f'(k)}{\omega^2 + f^2(k)}.
\end{aligned}$$

Now take the logarithm of both sides and using the approximation  $\log(1+x) \approx x$  for small  $x$ , we have approximately

$$\log(P^2) \approx \log(|D(N)|^2) + \sum_{k=1}^{N'} \frac{2(1 - \bar{\delta}_k)f(k)f'(k)}{\omega^2 + f^2(k)}. \quad (15)$$

We now approximate the sum in (15) by an integral, so that

$$\log(P^2) \approx \log(|D(N)|^2) + \int_{k=1}^{N'} (1 - \bar{\delta}_k) \frac{2f(k)f'(k)}{\omega^2 + f^2(k)} dk. \quad (16)$$

Making a change of variable from  $k$  to  $f$ , gives

$$\log(P^2) \approx \log(|D(N)|^2) + \int_{W_{p,1}}^{W_{p,N'}} (1 - \bar{\delta}(f)) \frac{2f df}{\omega^2 + f^2} \quad (17)$$

We look at the special form that the above equation takes when  $p = 1/2$ . In this case, from the results of the last section, we know that  $\bar{\delta}_k$  is very close to being constant at  $1/2$ , so that in (17) we have  $1 - \bar{\delta} = 1/2$ . We can then integrate the expression for  $P$  exactly to give

$$\log(P^2) \approx \log(|D(N)|^2) + \frac{1}{2} \log \left( \frac{(W_{p,N'})^2 + \omega^2}{(W_{p,1})^2 + \omega^2} \right)$$

so that

$$P \approx |D(N)| \left( \frac{(W_{p,N'})^2 + \omega^2}{(W_{p,1})^2 + \omega^2} \right)^{\frac{1}{4}}.$$

In this *critical case* it is equally likely that we will/will not have percolation paths at both small and large values of  $\omega$ . Accordingly, we must consider four equally likely cases of the distribution of the poles and zeros which could arise in any random realisation of the network. Thus to obtain the four possible responses of the network, we must now consider the contribution of the first zero and also of the last zero.

**Case 1:** First zero at the origin, last zero at  $N' + 1$

In this case we multiply  $P$  by  $\omega$  to give  $|Y_1|(\omega)$  so that

$$|Y_1(\omega)| \approx |D(N)_1| \omega \left( \frac{(W_{p,N'})^2 + \omega^2}{(W_{p,1})^2 + \omega^2} \right)^{\frac{1}{4}} \quad (18)$$

**Case 2:** First zero not at the origin, last zero at  $N' + 1$ .

In this case we multiply  $P$  by  $\sqrt{W_{z,1}^2 + \omega^2}$  to give  $|Y(\omega)|$ . We also use the result from the previous section that asymptotically  $W_{z,1}$  and  $W_{p,1}$  have the same form. This gives

$$|Y_2(\omega)| \approx |D(N)_2| (W_{p,N'}^2 + \omega^2)^{\frac{1}{4}} (W_{p,1}^2 + \omega^2)^{\frac{1}{4}} \quad (19)$$

**Case 3:** First zero at the origin, last zero at  $N'$

In this case we multiply  $P$  by  $\omega$  and divide by  $\sqrt{W_{z,N'}^2 + \omega^2}$  to give  $|Y|$ . Exploiting the fact that asymptotically  $W_{p,N'} \sim W_{z,N'}$  we have

$$|Y_3(\omega)| \approx |D(N)_3| \frac{\omega}{(W_{p,N'}^2 + \omega^2)^{1/4} (W_{p,1}^2 + \omega^2)^{1/4}} \quad (20)$$

**Case 4:** First zero not at the origin, last zero at  $N'$

In this case we multiply  $P$  by  $\sqrt{W_{z,1}^2 + \omega^2}$  and divide by  $\sqrt{W_{z,N'}^2 + \omega^2}$  to give  $|Y(\omega)|$ . Again, exploiting the fact that asymptotically  $W_{p,N'} \sim W_{z,N'}$  we have

$$|Y_4(\omega)| \approx |D(N)_4| \left( \frac{(W_{p,1})^2 + \omega^2}{(W_{p,N'})^2 + \omega^2} \right)^{\frac{1}{4}} \quad (21)$$

We know, further, from the calculations in the previous section that for all sufficiently large values of  $N$

$$CR W_{p,1} \sim \frac{1}{N} \quad \text{and} \quad CR W_{p,N'} \sim N.$$

Substituting these values into the above formulae gives:

$$|Y_1(\omega)| \approx |D(N)| \omega \left( \frac{(N/CR)^2 + \omega^2}{(1/NCR)^2 + \omega^2} \right)^{\frac{1}{4}} \quad (22)$$

with similar formulae for  $Y_2, Y_3, Y_4$ . The values for the constants  $|D(N)|$  can, in each case, be determined by considering the mid range behaviour of each of these expressions. In each case, the results of the classical Keller duality theory [16] predict that each of these expressions takes the same form in the range  $1/N \ll CR \omega \ll N$  and has the scaling law given by

$$|Y_i(\omega)| \approx \sqrt{\frac{\omega C}{R}}, \quad i = 1, 2, 3, 4. \quad (23)$$

Note that this is a true emergent expression. It has a different form from the individual component power laws, and it is also independent of the percolation path types for low and high frequencies. It is precisely the expression expected from an infinite lattice with  $p = 1/2$  due to the Keller duality theorem [16], in that  $|Y|^2 = \omega C/R$  is equal to the product of the conductances of the two separate components. As we have seen, the origin of this expression lies in the effect of averaging the contributions of each of the poles and zeros (and hence the associated simple linear circuits) through the approximation of the sum by an integral. In the case of (say)  $Y_1$  we see that the mid-range form of the expression (22) is given by

$$|Y_1| = |D(N)| \frac{\sqrt{N\omega}}{\sqrt{CR}}.$$

This then implies that  $|D(N)| = C/\sqrt{N}$  so that

$$|Y_1(\omega)| \approx \frac{\omega C}{\sqrt{N}} \left( \frac{(N/CR)^2 + \omega^2}{(1/NCR)^2 + \omega^2} \right)^{\frac{1}{4}} \quad (24)$$

Very similar arguments lead to the following expressions in the other three cases:

$$|Y_2(\omega)| \approx \frac{C}{\sqrt{N}} ((N/CR)^2 + \omega^2)^{\frac{1}{4}} ((1/NCR)^2 + \omega^2)^{\frac{1}{4}} \quad (25)$$

$$|Y_3(\omega)| \approx \frac{\sqrt{N}}{R} \frac{\omega}{((N/CR)^2 + \omega^2)^{\frac{1}{4}} ((1/NCR)^2 + \omega^2)^{\frac{1}{4}}} \quad (26)$$

$$|Y_4(\omega)| \approx \frac{\sqrt{N}}{R} \left( \frac{(1/NCR)^2 + \omega^2}{(N/CR)^2 + \omega^2} \right)^{\frac{1}{4}} \quad (27)$$

The four formulae above give a very complete asymptotic description of the response of the C-R network when  $p = 1/2$ . In particular they allow us to see the transition between the power-law emergent region and the percolation regions and they also describe the form of the expressions in the percolation regions. We see a *clear transition between the emergent and the percolation regions* at the two frequencies

$$\omega_1 = \frac{1}{NCR} \quad \text{and} \quad \omega_2 = \frac{N}{CR}. \quad (28)$$

Hence, the number of components in the system for  $p = 1/2$  has a strong influence on the *boundaries* of the emergent region and also on the *percolation response*. However the emergent behaviour itself is *independent of  $N$* . Observe that these frequencies *correspond directly to the limiting pole and zero values*. This gives a partial answer to the question, *how large does  $N$  have to be to see an emergent response from the network*. The answer is that  $N$  has to be sufficiently large so that  $1/NCR$  and  $N/CR$  are widely separated frequencies. The behaviour in the percolation regions is then given by the following

$$|Y_1(CR \omega \ll 1)| \approx \omega C \sqrt{N}, \quad |Y_1(CR \omega \gg 1)| \approx \frac{\omega C}{\sqrt{N}}. \quad (29)$$

$$|Y_2(CR \omega \ll 1)| \approx \frac{1}{\sqrt{NR}}, \quad |Y_2(CR \omega \gg 1)| \approx \frac{\omega C}{\sqrt{N}}. \quad (30)$$

$$|Y_3(CR \omega \ll 1)| \approx \omega C \sqrt{N}, \quad |Y_3(CR \omega \gg 1)| \approx \frac{\sqrt{N}}{R}. \quad (31)$$

$$|Y_4(CR \omega \ll 1)| \approx \frac{1}{\sqrt{NR}}, \quad |Y_4(CR \omega \gg 1)| \approx \frac{\sqrt{N}}{R}. \quad (32)$$

We note that these percolation limits, with the strong dependence upon  $\sqrt{N}$  are exactly as observed in Section 2.

## 6 Comparison of the Asymptotic and Numerical Results for the Critical Case

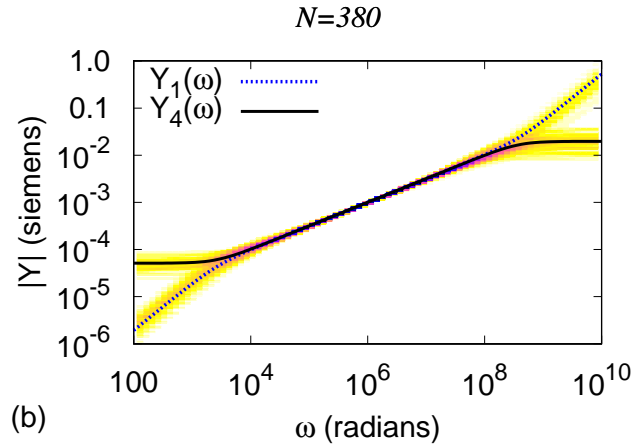
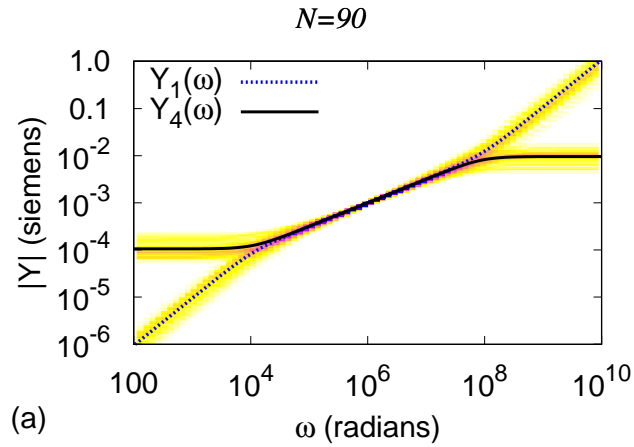
We can compare the four formulae (24,25,26,27) with the numerical calculations of the network conductance as a function of  $\omega$  for four different configurations of the system, with different percolation paths for low and high frequencies. The results of this comparison are shown in Figure 11 in which we plot the numerical calculations together with the asymptotic formulae for a range of values of  $N$  given by  $N = S(S-1)$  with  $S = 10, 20, 50, 100$ . We can see from this that the predictions of the asymptotic formulae (24,25,26,27) fit perfectly with the results of the numerical computations over all of the values of  $N$  considered. Indeed they agree both in the power law emergent region and in the four possible percolation regions. The results and the asymptotic formulae clearly demonstrate the effect of the network size in these cases.

## 7 Discussion

In this paper we have seen that the electrical network approximation to a complex disordered material has a remarkably rich behaviour. In this we see both percolation behaviour (which reflects that of the individual components) and emergent behaviour which follows a power-law quite different from that of the original components. The analysis of this system has involved studying the statistical properties of the resonances of the response. Indeed we could argue that both the percolation and emergent power-law responses are *simply manifestations of this spectral regularity*. The agreement between the asymptotic and the numerical results is very good, which supports our claim, and shows a clear link between the system behaviour and the network size. We hope that this form of analysis will be applicable to many other complex systems. Many questions remain open, for example a rigorous justification of the observed spectral regularity and an understanding of the relationship between the network model approximation and the true behaviour of the disordered material.

## References

1. P. W. Anderson. More is Different. *Biology and Computation: A Physicist's Choice*, 1994.
2. R. Bouamrane and D. P. Almond. The emergent scaling phenomenon and the dielectric properties of random resistor–capacitor networks. *Journal of Physics, Condensed Matter*, 15(24):4089–4100, 2003.
3. J. P. Clerc, G. Giraud, J. M. Laugier, and J. M. Luck. The electrical conductivity of binary disordered systems, percolation clusters, fractals and related models. *Adv. Phys.*, 39(3):191–309, Jun 1990.



4. B. Vainas, D. P. Almond, J. Luo, and R. Stevens. An evaluation of random RC networks for modelling the bulk ac electrical response of ionic conductors. *Solid State Ionics*, 126(1):65–80, 1999.
5. K. D. Murphy, G. W. Hunt, and D. P. Almond. Evidence of emergent scaling in mechanical systems. *Philosophical Magazine*, 86(21):3325–3338, 2006.
6. Jeppe C. Dyre and Thomas B. Schröder. Universality of ac conduction in disordered solids. *Rev. Mod. Phys.*, 72(3):873–892, Jul 2000.
7. KL Ngai, CT White, and AK Jonscher. On the origin of the universal dielectric response in condensed matter. *Nature*, 277(5693):185–189, 1979.
8. A. K. Jonscher. The universal dielectric response. *Nature*, 267(23):673–679, 1977.
9. K. Funke and R.D. Banhatti. Ionic motion in materials with disordered structures. *Solid State Ionics*, 177(19-25):1551–1557, 2006.

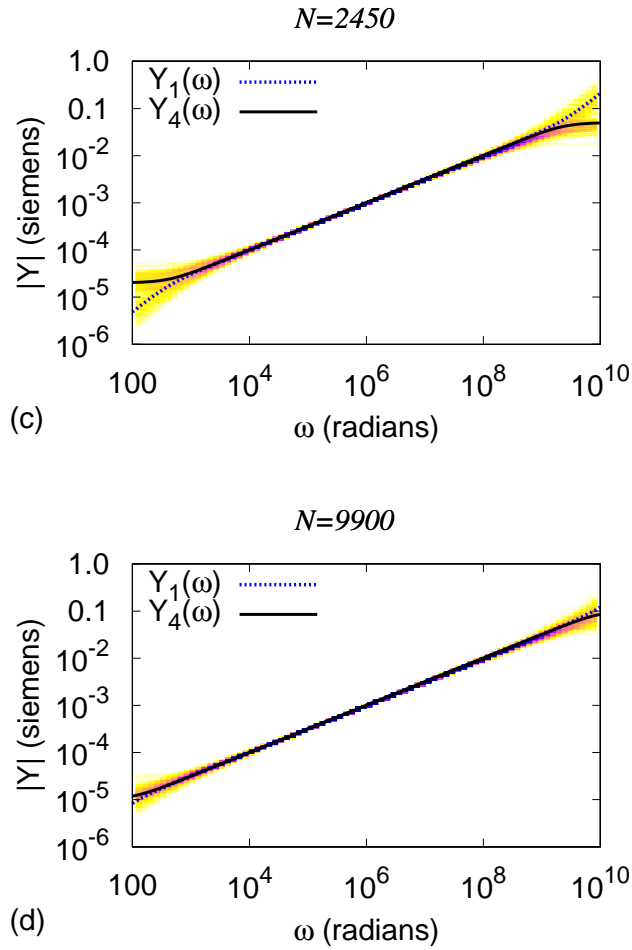


**Fig. 11.** Comparison of the asymptotic formulae with the numerical computations for the  $C - R$  network over many runs, with  $p = 1/2$  and network sizes sizes  $S = 10, 20, 50, 100$ ,  $N = S(S - 1)$ .

10. A. K. Jonscher. *Universal Relaxation Law: A Sequel to Dielectric Relaxation in Solids*. Chelsea Dielectrics Press, 1996.
11. C. Brosseau. Modelling and simulation of dielectric heterostructures: a physical survey from an historical perspective. *J. Phys. D: Appl. Phys.*, 39:1277–94, 2005.
12. V.-T. Truong and J. G. Ternan. Complex Conductivity of a Conducting Polymer Composite at Microwave Frequencies. *Polymer*, 36(5):905–909, 1995.
13. T. Jonckheere and JM Luck. Dielectric resonances of binary random networks. *J. Phys. A: Math. Gen.*, 31:3687–3717, 1998.

14. S. R. Broadbent and J. M. Hammersley. Percolation processes. I, II. *Proc. Cambridge Philos. Soc.*, 53:629–641, 1953.
15. C.D. Lorenz and R.M. Ziff. Precise determination of the bond percolation thresholds and finite-size scaling corrections for the sc, fcc, and bcc lattices. *Physical Review E*, 57(1):230–236, 1998.
16. G. W. Milton. Bounds on the complex dielectric constant of a composite material. *Applied Physics Letters*, 37:300, 1980.